mAbs ›
Volume 5, 2013 - Issue 3

Free access



Report

# A fully synthetic human Fab antibody library based on fixed VH/VL framework pairings with favorable biophysical properties

Thomas Tiller, Ingrid Schuster, Dorothée Deppe, Katja Siegers, Ralf Strohner, Tanja Herrmann, ...show all

Pages 445-470 | Received 12 Dec 2012, Accepted 06 Mar 2013, Published online: 09 Apr 2013

Cite this article https://doi.org/10.4161/mabs.24218





## Abstra

This rep synthetic human F ed immuno ch cover a broad ures. The varia cal characte process included thermal stability IgG1 formats, fixed and the dive ge set of rearrang currence of

performed against various antigens and unique antibodies with excellent biophysical properties were isolated. Our results confirm that quality can be built into an antibody library by prudent selection of unmodified, fully human VH/VL pairs as scaffolds.

Keywords: : antibody engineering | human antibody library | phage display | Slonomics | CDR-H3 design | VH/VL pairing | Ylanthia

## Introduction

Due to their high specificity and broad target space, monoclonal antibodies (mAbs) represent the most important class of biologics and have great potential for both diagnostic and therapeutic applications.[1] A diverse set of in vivo and in vitro technologies are currently available for the generation of these versatile molecules. Fully human mAbs, for example, can be derived from human B cells by immortalization via viral transformation,[2] through the generation of human hybridomas,[3] or through direct cloning of Ig encoding gene transcripts.[4-6] Target specific human B cell material, however, in some cases may not be readily accessible. The hybridoma technology[7] using immunoglobulin (Ig) transgenic mouse systems[8] overcomes this limitation but still suffe unogenic sequenc s share the advanta h naturally paired a neworks.

Among t f human mAbs ar ries.[9-14] Various r rmats have been osition and comp r quality, as defined lisplay include t cteristics (e.g., im a wide range of ies for animal r logical robustne

Therapeutic antibodies must fulfill high standards with regard to their binding affinity, target and epitope specificity, and functional activity. An additional challenge of antibody discovery technologies is the generation of mAbs with appropriate biophysical properties. To reach the market, antibody therapeutics ideally should, for example, not aggregate or precipitate and resist degradation by proteases, as these factors contribute to optimal manufacturing and shelf life properties and ensure a long serum half-life. Furthermore, the increasing demands of regulatory authorities with respect to properties such as the homogeneity of the product drive these needs. Similar stability requirements also apply for diagnostic and research mAb tools.[24]

Various approaches have been undertaken to combine the advantages of in vivo and in vitro technologies to generate recombinant libraries that include predominantly antibodies with superior properties. For example, the human combinatorial antibody library (HuCAL) platform is based on a composition of selected VH and VL consensus master gene sequences that are diversified using modular CDR cassettes.[19] HuCAL PLATINUM, the latest generation HuCAL antibody library,[20] implemented optimized antibody framework sequences with a reduction of unproductive sequences and a revised rational CDR design compared with the previous HuCAL scFv and HuCAL GOLD libraries.[19,21] Another approach to combine structural CDR diversity with a biophysically optimal VH/VL combination is the n-CoDeR scFv antibody library, which uses a VH3–23/Vλ1–

The Ylan L framework pairs are elevant for antibody optimal biophysi ntibody sequenc ow leading to the fi irst, 20 VH, 12 V the human antibo DR structure 40 variable domains ng to properti bility, aggrega levels on phage. A rs were

pairs, high structural diversity is maintained as important basis for selecting antibodies against a broad range of different epitopes and target classes.

The CDR-H1 and CDR-H2 design of these 36 VH/VL framework pairs was based on germline-encoded CDR sequences. Diversity was introduced to remove potential post-translational modification sites (PTMs) (e.g., deamidation sites Asn-Ser, NS; Asn-Gly, NG; Asn-His NH; isomerization sites Asp-Ser, DS; Asp-Gly, DG; Asp-Asp,DD; protease cleavage sites Asp-Pro, DP; Asp-Glu, DQ; oxidation sites Met, M)[26] within CDR-H1 and CDR-H2 in a significant proportion of the library. To enhance antibody Fab expression in bacterial and IgG expression in mammalian systems, nucleotide sequence codon optimization was implemented during library construction.[27] The use of the TRIM[28] and the Slonomics[29] technology to engineer diversified CDR-L3 and CDR-H3 cassettes, respectively, allowed for sophisticated CDR design and guarantees a very high proportion of correct clones. The amino acid diversity of the CDR3 cassettes was based on the Ig gene segment- (CDR-L3) and on the CDR length (CDR-H3) to mimic the natural position-dependent occurrence of amino acids in the CDR3s with a strong reduction or omission of potential PTMs.

To confirm the functionality and quality of the Ylanthia antibody library, phage selections on recombinant human (rh) TNF-α, M-CSF, rhErbB4, rhFZD-4, eGFP and several other antigens were performed. Selected Fab fragments were converted into full-leng ical properti translate into high avorable biophysi

## Result

### Anal

To asses referentially occurrin enerated data we th healthy and auto ted IgM (n = 1348), s re combined

information was gained experimentally from single mature naïve B cells and antibody secreting cells isolated from a healthy donor. In total, 2138 VH, 1358 Vκ and 780 Vλ functionally rearranged sequences were included in the analysis of VH/VL pairing frequency. Additional, 326 VH[36,37] and 298 Vκ[38] productive sequences were utilized in the ranking of the most frequently used VH and Vκ gene segments.

VH3–23 (10.6%) and VH3–30 (8.0%) gene segments were found to be the most frequent among the analyzed human VH sequences, followed by three members of the VH4 gene family, VH4–39 (7.6%), VH4–34 (6.8%) and VH4–59 (5.8%) as well as VH1–69 (5.3%). Within the human Vκ sequences Vκ3–20, Vκ1–39, Vκ1–5, Vκ3–15 and Vκ4–1 together constituted more than 60% of all analyzed Vκ sequences. Vλ2–14 was the most frequently found Vλ gene segment (18.1%), followed by Vλ1–40 (11.3%), Vλ1–44 (11.3%) and Vλ1–51 (10.0%) (Fig. 1).

Figure 1. Frequency distribution of (A) VH, (B) Vκ and (C) Vλ gene segments in the natural human antibody repertoire. V gene usage for human antibodies was compiled from several B cell repertoire studies [30-38] and own sequencing efforts as described in the methods section. The names of the most frequent V segments are listed in the respective boxes, less frequent used V segment groups are indicated by *(VH1–3, VH1–8, VH1–24, VH1–58), **(VH3–13, VH3–20, VH3–43, VH3–49, VH3–64, VH3–66, VH3–72, VH3–73, VH3–74), ***(VH4–28, VH4–30-2, VH4–61), ****(VH2–5, VH6–1, VH7–4.1, VH7–81), #(V[illegible]7, Vκ1D-43), ##(Vκ2-[illegible]D-11, Vκ3D-15, Vκ3D[illegible]λ3–12, Vλ3–19, Vλ3-[illegible]7–46, Vλ8–61, Vλ9-

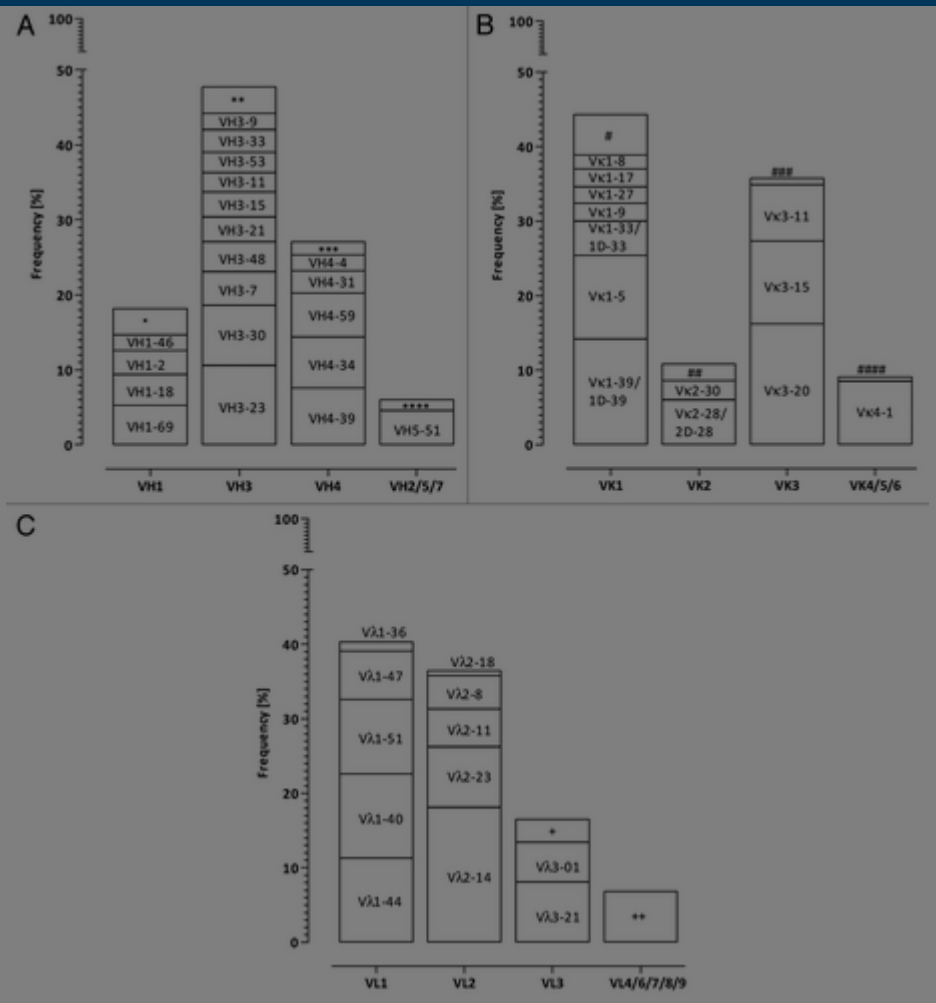


Display full size

The most prevalent natural VH/VL pairs were primarily composed of the most frequent with previous ing of certain g lambda ( Fig. 3) a 3 VH/Vκ and 311 VH/ ations have been fou

Figure 2. an antibody repe yzed VH/Vκ sequ ed accordin ubble size refers to les indicate the 240 heir absolute es and frames s The circles indicate ir

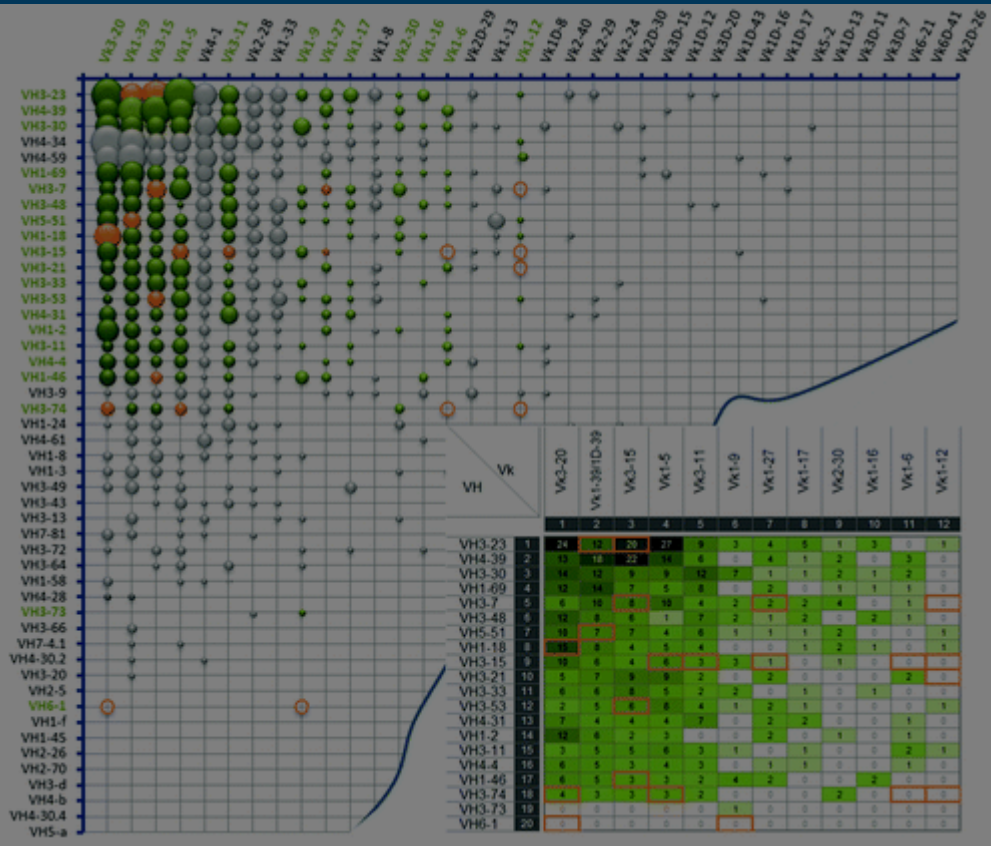


Display full size

Figure 3. Frequency distribution of VH/Vλ antibody pairs in the natural human antibody repertoire. Bubble chart illustrating VH/Vκ pairing frequencies of 780 analyzed VH/Vλ sequences from the natural human antibody repertoire. V segments are listed according to their individual frequency in the Ig lambda antibody pool. Each bubble size refers to es indicate the 160 heir absolute es and frames s The circles indicate ir sequenc

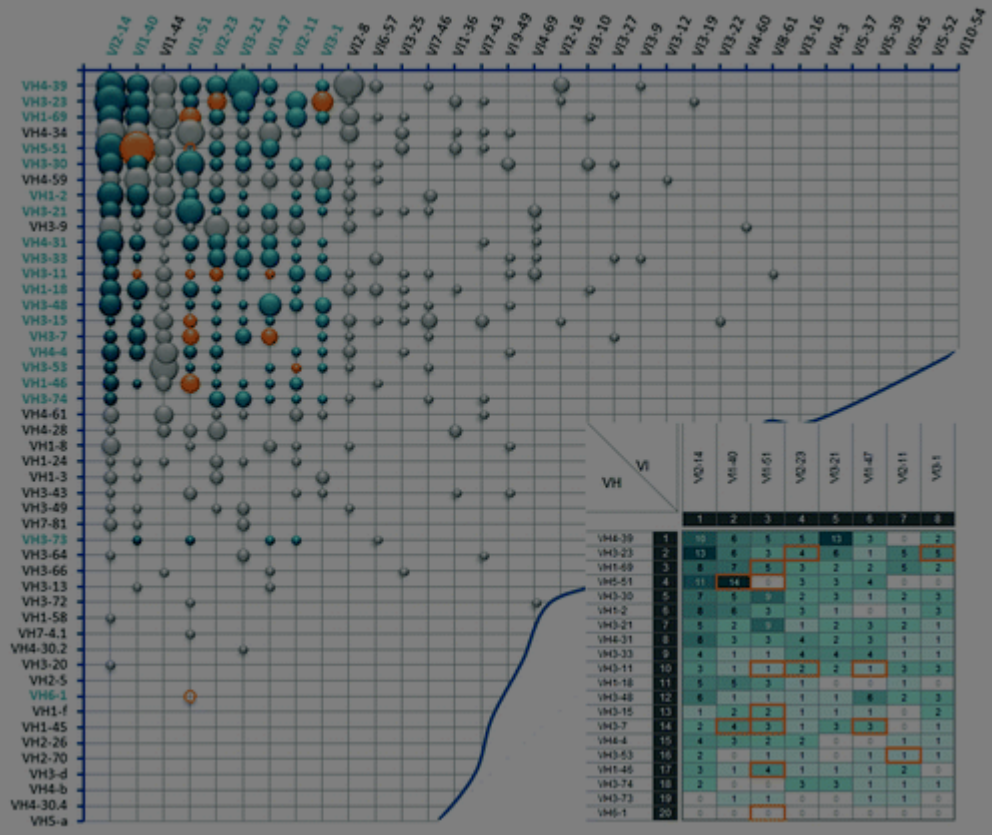

Display full size

An in-depth in silico and experimental in vitro analysis was performed to identify germline VH/VL pairs that are ideally suited as frameworks for this novel type of antibody library. While the focus was to identify VH/VL pairs with superior biophysical properties, care was also taken to maintain diversity in Ig V gene segment families and canonica

## In silic ments

Unpaire 5%, 1% and 5% of th in silico in their ge (pI), 2) CDR1 ar d free cyst t VH, Vκ and Vλ seq pertoire, for examp ibodies have been fou ore, antibod The VH3–9 sequenc overrepr on, the less

diversity of canonical CDR-H structures. The prominent Vκ and Vλ gene segments, Vκ4–1, Vκ2–28/2D-28, Vκ1–33/1D-33, Vκ1–8, Vκ2D–29 and Vλ1–44 were also excluded for the reasons described above[20,43] and to prevent an overrepresentation of Vκ1 and Vλ1 family sequences.

Table 1. In silico analysis of selected V gene element amino acid sequences

Download CSV | Display Table

The isoelectric point (pI) of a therapeutic antibody is an important aspect for formulation development. Values of pIs in the range of the pHs commonly used for antibody formulation, i.e., in the physiological or slightly acidic range, can be problematic due to a potentially increased propensity of such antibodies to aggregate under these conditions. Within the selected VH gene segment sequences, the calculated pI values ranged from 8.0 (VH3–48) to 9.5 (VH3–73). In the analyzed Vκ gene segment sequence pool the observed pI values were between 5.0 (Vκ1–5) and 8.7 (Vκ1–17, Vκ1–27). The selected Vλ gene segments displayed the lowest pI values ranging from 4.5 (Vλ3–1) to 6.7 (Vλ2–11, Vλ2–23).

All classi… (H2–1, H2–2, H2–3, …Vκ and Vλ CDR-L1, …ble 1). The majority … PTM sites. Of the a… VH1–69 had no s… genes, however… NxS and Asn-Xaa… nt in the germ… e segments. They ca…

Through… rmline sequenc… e frequency of natura… DR structure… house in vitro ant… otential PTM

sites were considered to be important aspects as they might hamper later manufacturing and development steps.

## In vitro screening of VH/VL pairs in Fab and human IgG1 format

The selected 20 VH, 12 Vκ and 8 Vλ gene segments were combined to generate VH/VL pairs for experimental analysis. A set of predictive screening assays was performed as described below to reduce the number of VH/VL pairs for subsequent, more detailed analysis.

The 400 VH/VL pairs resulting from the combination of the 20 VHs with 20 VLs represent the most prominent VH/VL pairs in the human antibody repertoire (Figs. 2 and 3). During testing, all VH regions carried the same CDR-H3, which is derived from the VH region of the hu4D5–8 antibody,[19,47] and all VL regions carry a kappa-like and lambda-like CDR-L3, respectively.[48]

## Relative expression yields of Fab and IgG1 VH/VL pairs

Of the theoretically possible 400 VH/VL combinations, 285 different VH/VL pairs were identified following a pooled cloning approach. They were analyzed for relative Fab expression in bacterial cell lysates by ELISA (Fig. 4), where the expression level of each VH/VL pair was determined relative to the expression of the reference Fab VH1–69/Vλ1–40. More ion of at least 0.4 the highest relative her VH families, ested VH/VL Fab pairs st relative expressi observed for these fra ork showed a low 0.47 vs. 0.78, g (Fig. 4C).

Figure 4. by ELISA. (A) VH, ( shown compare an with interqua tes with relative 36 VH/VL

pairs that are included in Ylanthia. The circles indicate VH/VL pairs that were not determined.

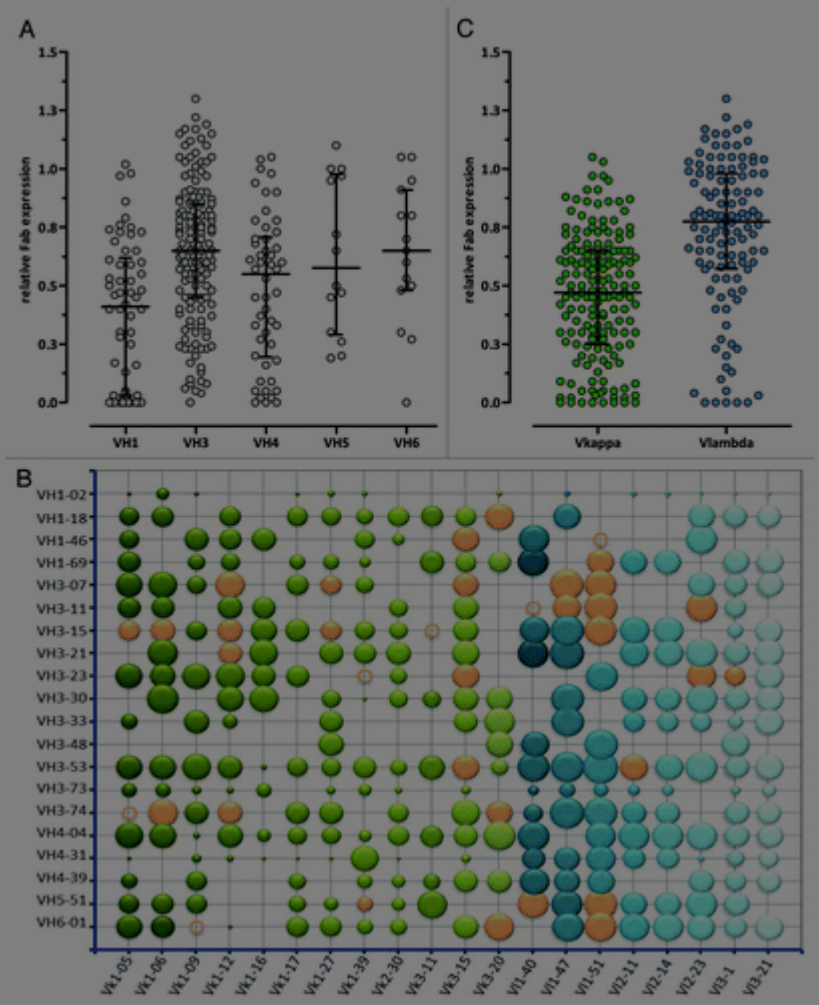


Display full size

For hum gG1 expressi ds. In this way, all IgG1 expressi n yields were cal gnal of a high lev tested VH/V evel of the refere urprisingly, all VH1– compared with the median IgG1 exp vs. 0.5, p = 0.59, Ma Fab and mamma

Figure 5. Relative expression levels of different VH/VL IgG1 pairs determined by ELISA. (A) VH, (B) VH/VL and (C) VL (Vκ: green, Vλ: blue) relative production yields are shown compared with a high expressing internal reference IgG1 antibody. In (A) and (C) the median with interquartile range is shown, in the bubble chart (B) the bubble area correlates with relative IgG1 expression. Orange bubbles and circles show the final selected 36 VH/VL pairs that are included in Ylanthia. The circles indicate VH/VL pairs that were not determined.

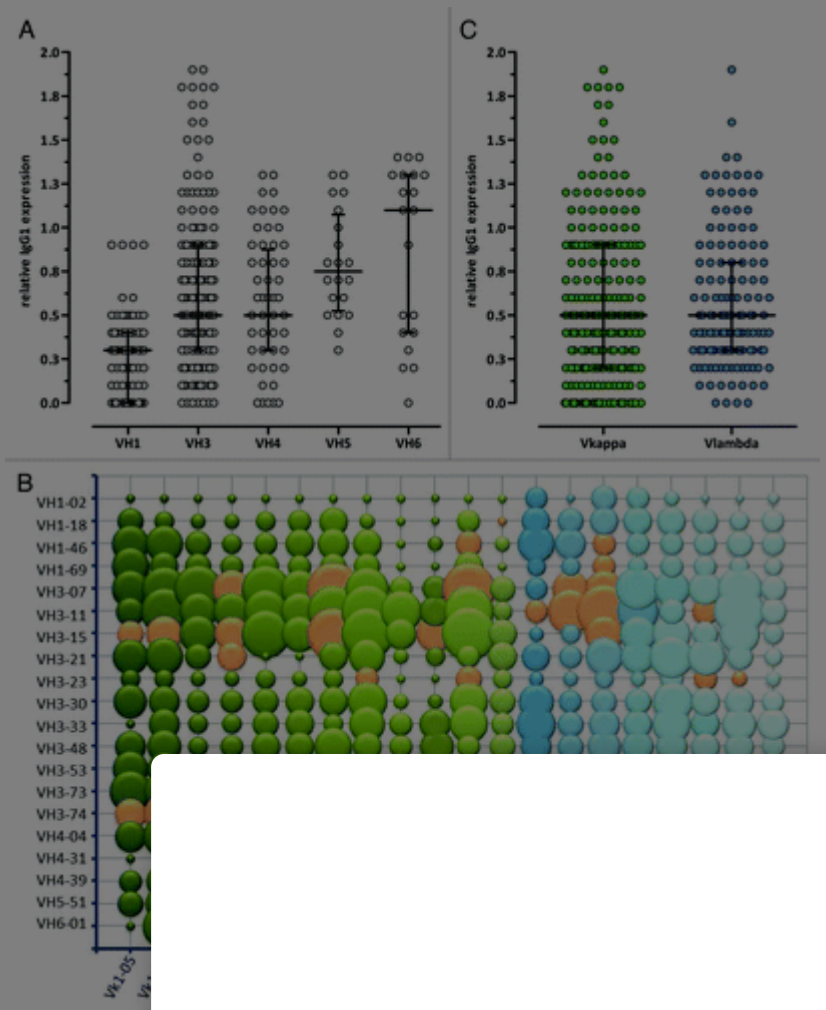


Display ful

## Relativ

To er ge pannings, 243 VH/ nage by ELISA (Fi as significa ay rates of VH1 (1.9 VH3 vs. VH1, VH3 vs. < 0.05, one-way ana Within the

Article contents | Related research

phage display rate (0.2). Low Fab display and expression were also observed for VH1–2, VH4–31, VH4–39 and VH5–51 containing VH/VL pairs (Fig. 6B). Between VH/Vκ and VH/Vλ pairs, no significant difference in relative Fab phage display rates was detected (median 4.4 vs. 4.6, p = 0.30, Mann–Whitney U-test) (Fig. 6C).

Figure 6. Relative display rates of different VH/VL Fab pairs determined by ELISA. (A) VH, (B) VH/VL and (C) VL (Vκ: green, Vλ: blue) relative display rates are shown compared with an internal reference phage preparation. In (A) and (C) the median with interquartile range is shown, in the bubble diagramm (B) the bubble area correlates with relative Fab display. Orange bubbles and circles show the final selected 36 VH/VL pairs that are included in Ylanthia. The circles indicate VH/VL pairs that were not determined.

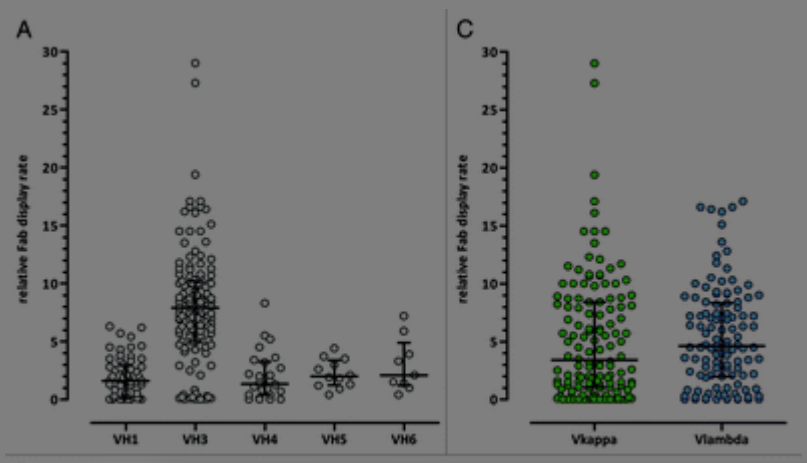




Therma

The app bility and resistanc lysates incubate lefined

conformation-sensitive antibodies for detection. Denatured, aggregated or degraded Fab molecules were expected to show reduced signals. Of the 285 tested Fab VH/VL pairs, 215 (75%) showed a Tm of at least 60°C. In addition, our results suggest that the majority of VH/VL combinations comprising Vκ1–17 and Vκ2–30 are not stable at temperatures above 60°C, whereas most VH/VL pairs containing Vκ1–27 and Vκ3–15 were stable at 70°C (data not shown). Although this experiment was not suited to determine the exact Tm of the Fab molecules, this screening approach allowed rapid identification of VH/VL pairs sensitive to elevated temperatures.

In conclusion, the screening results showed that VH/VL framework pairs differ in their relative Fab display rate on phage, their Fab and IgG1 expression levels and thermal stability in vitro. This combined experimental data set was used as a basis for selecting 95 promising VH/VL pairs for further detailed characterization. The previous screening assays were useful in identifying VH/VL pairs containing instable Ig light chains, such as Vκ1–17 and Vκ2–30 or low expressing Ig heavy chains, e.g., VH1–2 and VH3–73. Such Ig heavy and Ig light chains were consequently excluded from all further evaluations.

## Biophysical characterization of pre-selected Fab and IgG1 VH/VL pairs

On the basis of these screening results, 95 VH/VL pairs were selected for a more detailed analysis. This detailed examination of purified VH/VL pairs included the quantific levels, the analysis s a pH and physical ring manufac

## Resear

The synt ed[27] for both ab and IgG1 expre esearch-scale Fal nged from 1.5–13 n ll lysate Fab expressi major differenc nd Vλ bearing -selection of well-exp 00. Mann–

mg/L, with only VH/ Vλ3–1 pairings showing relatively low expression levels (Fig. 7A, left). VH/VL combinations in human IgG1 format showed moderate to high expression yields in HKB11 cells ranging from 20–80 mg/L with a median yield of 49.5 mg/L. Again, no significant difference in expression levels was detected between Vκ and Vλ bearing VH/VL IgG1 pairs (median 46.6 vs. 46.6, p = 0.5, Mann–Whitney U-test) (Fig. 7A, right).

Figure 7. Biophysical features of human Fab and IgG1 VH/VL pairings. (A) Production yields of purified Fab (left panel) and human IgG1 (right panel) molecules after purification as determined by UV-spectrophotometry. (B) Monomer contents of purified Fab (left panel) and human IgG1 (right panel) molecules as determined by SEC. (C) Apparent melting temperatures of purified Fab (left panel) and human IgG1 (right panel) molecules as determined by DSF measurements. In each panel the median with interquartile range is indicated. VH/Vλ3–1 pairs are highlighted as red squares.

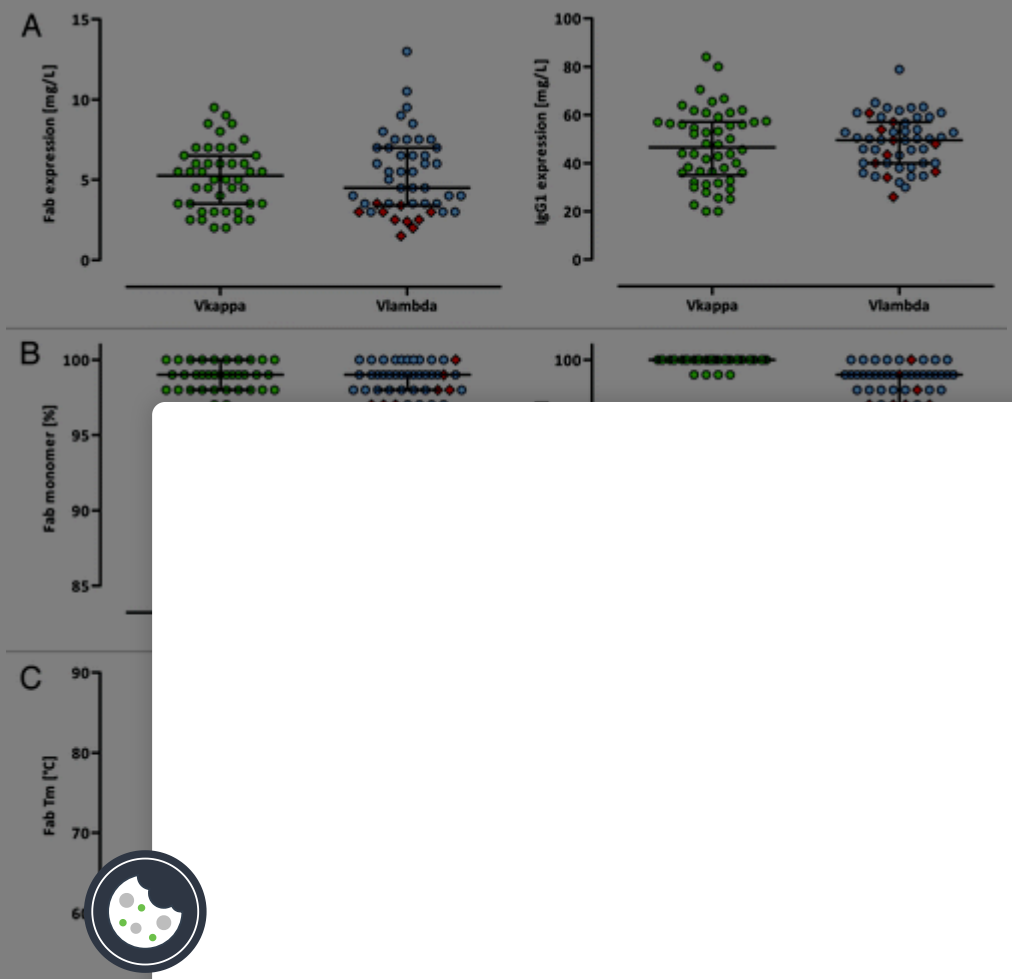




## Aggreg

The pres s following purificat

between 88% and 100% with a median monomer portion of 99% each for VH/Vκ and VH/Vλ Fab fragments and VH/Vλ IgG1 molecules. VH/Vκ IgG1 antibodies showed a median monomer content of 100%. Compared with Vκ combinations, Vλ bearing Fab and IgG1 VH/VL frameworks seem to be more prone to aggregation (Fab: $p = 0.03$, Mann–Whitney U-test, Fig. 7B, left; IgG1: $p < 0.0001$, Mann–Whitney U-test, Fig. 7B, right). The vast majority (96%), however, showed monomeric portions above 95%, indicating a very low aggregation tendency. Furthermore, electrophoresis-based analyses under denaturing reducing conditions demonstrated purities above 92% (data not shown) with no precipitations occurring during the purification process.

## Melting temperatures (Tm) of purified Fab and IgG1 VH/VL pairs

The apparent Tms of the purified Fab molecules determined by differential scanning fluorometry (DSF)[50-52] ranged from 50.9°C (VH3–07/Vλ3–1) to 77°C (VH3–15/Vκ3–15) with a median Tm of 74.0°C for Vκ and 72.4°C for Vλ containing frameworks ($p < 0.0001$, Mann–Whitney U-test, Fig. 7C, left). In addition, the second transition Tms of the IgG1 antibodies, which represents the stability of the Fab portion, ranged from 69.7°C (VH3–07/Vλ3–1) to 85.0°C (VH3–23/Vκ3–15) with a median Tm of 78.4°C and 78.5°C for Vκ and Vλ IgG1 combinations, respectively ($p = 0.68$, Mann–Whitney U-test, Fig. 7C, right). The human IgG1 Fc domain shows a transition between 68.4 and 70.6°C (data not shown). In cases with only one single transition, the Tm of the Fab portion coincide 1 pairs of Ylanthia °C.

The Tm fter acidic stress ex by pH-stress co e selected Fab and unfolding after

## Molecu

To study odynamic radius a scattering (DLS). O s showed a hydrody to exist as monome 46/Vλ3–21

between 7 and 14 nm and two framework pairings (VH6–1/Vλ1–47 and VH6–1/Vλ3–1) exhibited a radius higher than 20 nm, indicating the presence of higher molecular weight aggregates (Fig. 8). Interestingly, the Vλ3–1 framework is present prevalently within these VH/VL pairs.

Figure 8. Polydispersity of purified human IgG1 antibodies. The hydrodynamic radius of purified VH/VL IgG1 molecules was determined by DLS experiments. VH/Vλ3–1 pairs are highlighted as red squares.

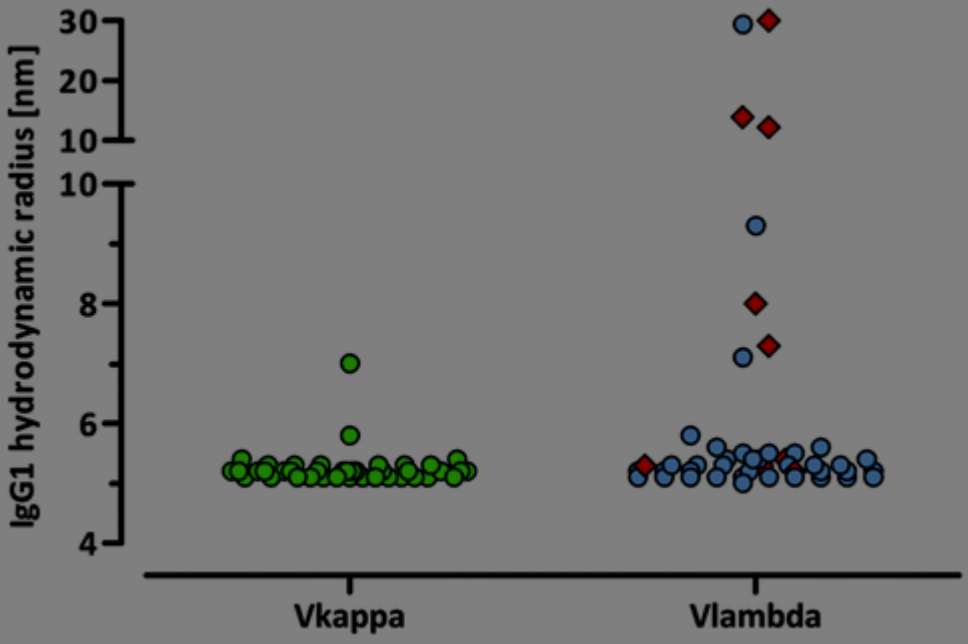


Display ful

For the r ered after
acidic tr higher than
7 nm be adius after
acidifica

The initi 0% with 11
antib geneity. For 6
out o
heteroge an increase
in sampl on or
conform

## Turbidi

UV-spect e turbidity

acidification and subsequent neutralization. Except for three VH/VL pairs (VH1–46/Vλ3–1, VH6–1/Vλ1–47, VH6–1/Vλ3–1) that already showed a relatively high initial extinction, all other tested VH/VL pairs showed no or only a moderate increase in turbidity upon low pH treatment, indicating a relative resistance toward aggregate formation. The morphology of visible and sub-visible aggregates in solution was further assessed by a semi-quantitative particle staining assay (data not shown).

## Library composition, CDR3 design and library cloning

Based on the above analyses, 36 VH/VL framework pairs with good expression and display properties and superior biophysical features were selected as frameworks for the Ylanthia library. An overview of the biophysical data of the finally selected 36 VH/VL framework pairs is given in Table 2A and Table 2B.

### Table 2A. Igk VH/VL pairings that constitute the final Ylanthia antibody library

Download CSV | Display Table

### Table 2B. Ig λ VH/VL pairings that constitute the final Ylanthia antibody library

Downlo

The 36 s e segments. As the Ig tential PTM hot spot e segments contain R-H2s that have

In contra 21 and HuCAL P ations of VH and VL d nd CDR-H3 diversity rtoire were closely r d in the design f R-L3s, the

were realized. The composition of each CDR-L3 cassette was designed according to the corresponding VL gene segment region that naturally contributes to CDR-L3.

Natural CDR-H3 diversity is mainly generated by VDJ recombination of different VH, D and JH gene segments that result in CDR-H3 sequence length variations from a few to more than 30 amino acids.[53] In Ylanthia, 12 different CDR-H3 lengths ranging from 6 to 17 amino acids were implemented. These CDR-H3 lengths cover about 80% of naturally occurring CDR-H3 sequences as described by Zemlin and coworkers.[53] The CDR-H3 length and amino acid composition design was identical for all VH gene segments used. It has been observed that JH4 is used predominantly in rearranged human antibodies and that the incorporation of the longest JH6 gene segment gains importance with increasing CDR-H3 lengths, resulting in subtle differences in positional amino acids diversities.[53] Therefore, the realized amino acid composition in the CDR-H3 is based on naturally rearranged Ig sequences using JH4, where the composition of the lengths 12 to 17 amino acids has an additional JH6-based design closely reflecting the CDR-H3 length-dependent amino acid frequencies in the human antibody repertoire.

To abolish or reduce the occurrence of potential critical PTM sites in the CDR-L3 and CDR-H3, the amino acids asparagine (Asn, N), aspartic acid (Asp, D) and methionine (Met, M) were decreased or completely omitted, as, for example, in the case of Asn in CDR-H3 sequences. The overall CDR-H3 design is schematically illustrated in Figure 9.

Figure 9

cids at each position

and amino acid freq

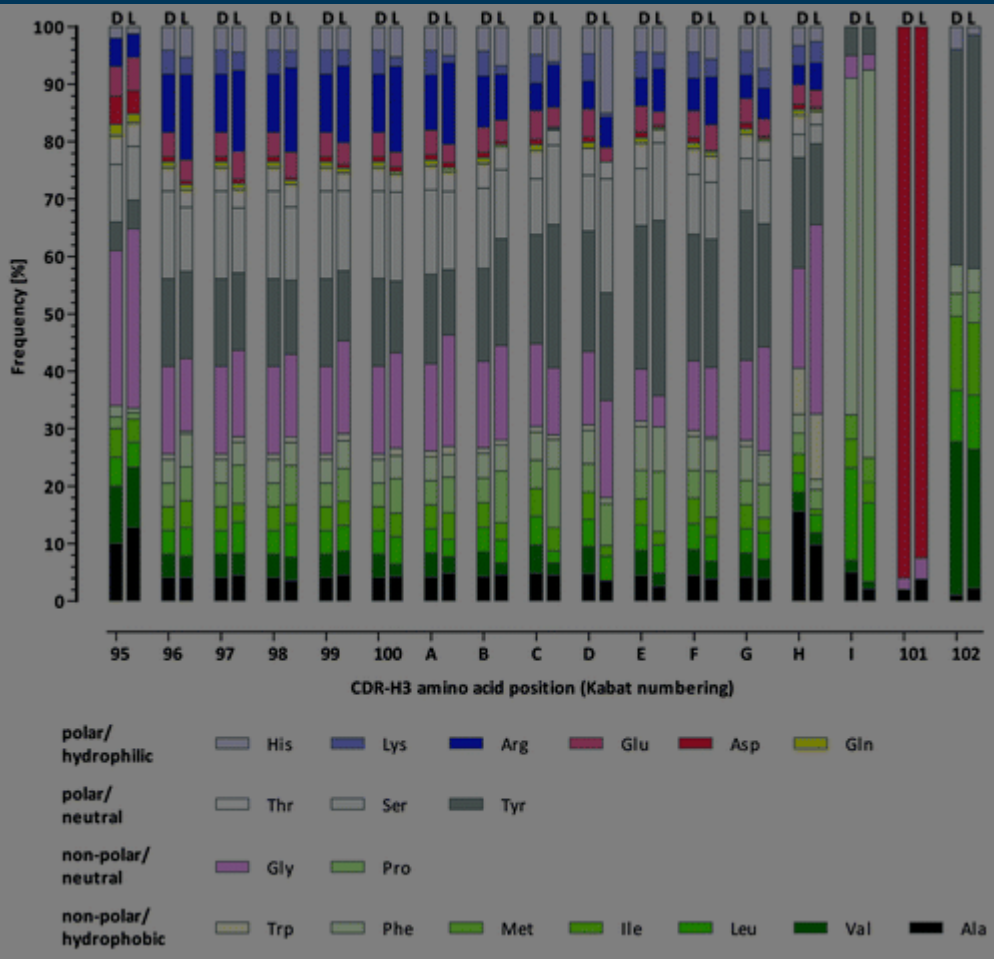


Display full size

## Library size, sequence correctness and diversity

The theo m 3.8E+06 to 2.5E+ rary size of 5-fold ab ies, the size was rest the VH/VL pairs we -08 to 4.4E+09 s.

The qua during the cloni efined by corre e diversified CDR-L3 ol (QC) was perform ssettes, prior to their i nfirmed the VL seque assettes). VL sequenc ter the final cloning s performed

sequence correctness of the intermediate Ig light chain sub-libraries was 85% for all Ig lambda and 86% for all Ig kappa sub-libraries. After the insertion of the CDR-H3 cassettes in the second cloning step, the CDR-L3 sequence correctness remained unchanged and the average CDR-H3 correctness alone of all sub-libraries was 90% resulting in a combined CDR-L3 and CDR-H3 sequence correctness of at least 82% for each sub-library.

The initial CDR-L3 and CDR-H3 QC also included the comparison of the amino acid composition of each variable position synthesized with that of the library design. As shown in Figure 9, no major deviations between the observed composition in the unselected library and the library design were observed for the CDR-H3 lengths 6 to 17 for roughly 4,000 analyzed sequences. In addition, the CDR-H3 length variability observed in the library prior to antigen selection very closely mirrored the expected length distribution (Fig. 10).

Figure 10. CDR-H3 length distribution in Ylanthia. CDR-H3 lengths according to the library design (white bars) and as determined after small QC (gray bars, analysis of ~3,200 sequences) and after 454 sequencing (black bars, analysis of > 152,000 sequences).

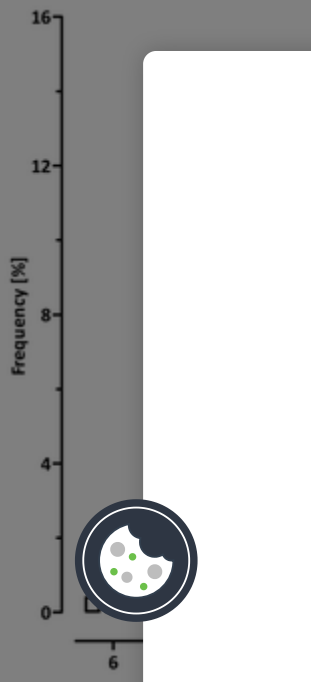




To furthe amework distribut s performed

data were evaluated using proprietary software tailored for analysis of large sequencing data sets. For CDR-H3 length analysis, a total of 160,521 high quality reads (> 300 bp) were generated, of which 152,365 could be assigned to a corresponding length-specific group. As shown in Figure 10, the CDR-H3 length distribution was congruent with the profile obtained in the small scale QC described above, with a slight reduction of the longest length variants. For codon-based CDR-H3 redundancy analysis, the occurrence of sequence replicates was compiled from the same data set (> 152,000 sequences). The complete library was found to be composed of 94% unique nonredundant antibody CDR-H3 sequences. The remaining ~6% of the library was found as duplicate CDR-H3 sequences (5.4%) and to a very low percentage as tri- and quadruplicates, which together accounted for 0.38% (Fig. 11). Importantly, CDR-H3 sequence diversity as defined by the ratio of the number of different sequences divided by the total number of sequences was greater than 97%.

Figure 11. Codon-based sequence redundancy in Ylanthia as determined by 454 sequencing. VH region sequences were amplified using pan-selective primers recognizing all Ig heavy chain sequences. From more than 152,000 analyzed VH sequences 94% were unique in their CDR-H3 with less than 6% of sequences found in duplicates, indicating high sequence diversity.

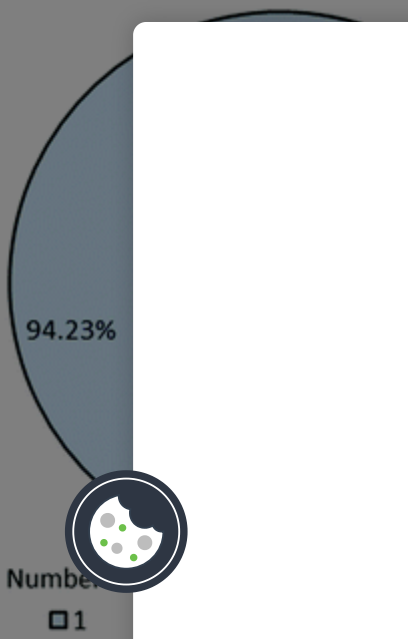


Display ful

Of note, s" CDR-H3 library a cing has not reveale eading to

the suggestion that the major portion of the observed replicates originates most likely from an amplification bias introduced during the 454 workflow.

For framework distribution analysis the frequencies of each VH, Vκ and Vλ framework were compiled from sequences (> 90bp) that could be unambiguously assigned to specific frameworks. For VH, Vκ and Vλ 130,983, 94,232 and 99,871 sequences, respectively were evaluated. The VH (Fig. 12A), Vκ (Fig. 12B) and Vλ (Fig. 12C) framework frequencies were found to the portions as expected by the design indicating an unbiased cloning performance during the construction of the Ylanthia library.

Figure 12. VH, Vκ and Vλ framework distribution in Ylanthia as determined by 454 sequencing. By analyzing more than 325,000 sequences in total, the observed distribution of the (A) VH (gray bars), (B) Vκ (green bars) and (C) Vλ (blue bars) frameworks closely represented the expected frequencies by design (white bars) in the library.

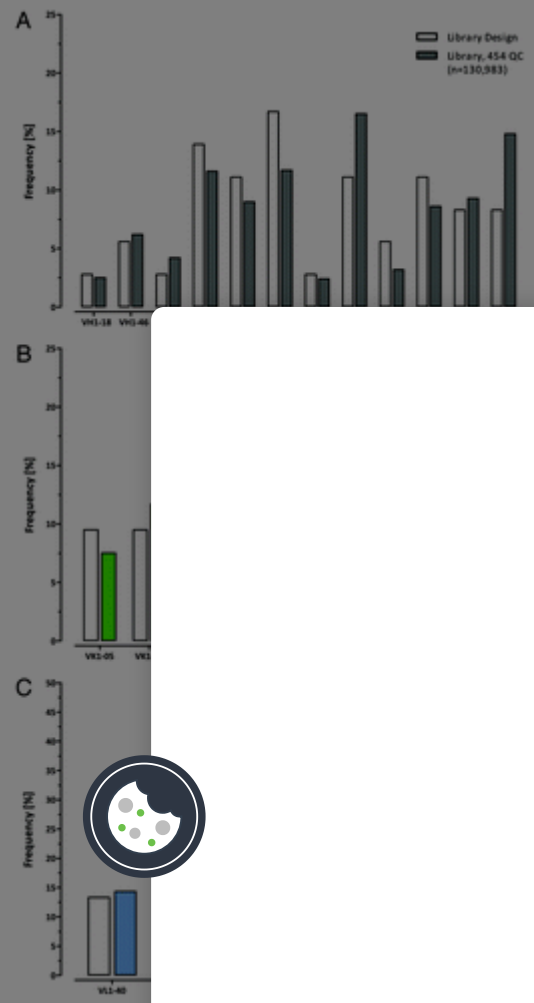




Antibo

Phage preparations for each sub-library were performed as outlined in the materials and methods section and phage titers and relative Fab display rates were determined by UV-spectroscopy and ELISA, respectively (data not shown). Antibody phage selections ('pannings') were performed according to standard protocols.[54,55] The following different protein antigens were used to perform phage selections: recombinant human (rh) ErbB4, rhFZD4/Fc, rhTNFalpha, M-CSF, eGFP, a human IgG1 antibody (with the goal to generate anti-idiotypic antibodies) and three other antigens. After three rounds of pannings, the enriched Fab encoding sequences were subcloned as pools into the pYBex10 Fab expression vector. Antigen-specific Fabs were identified by ELISA, where a positive hit was defined by binding to its specific target with a signal at least 5-fold above the assay background.[54,55] Overall, 2,900 to 5,200 clones were screened per target antigen with primary hit rates ranging from 1% to 49%. Sequencing of up to 785 positive hits revealed 7 to 284 CDR-H3 unique antibodies per antigen, although the total diversity of selected antibodies will most likely be much higher because only a minor fraction of the clonal panning output was screened and sequenced. Notably, a low hit rate was only observed with challenging targets, e.g., anti-idiotype selection, due to the relative scarcity of unique epitopes on the target antigen (binding interface of human IgG1 antibody). So far, antibodies from 27 distinct VH/VL combinations (out of 36 VH/VL pairings) were identified. Different target antigens thereby favor different VH/VL pairings (data not shown), arguing for increased framewo logies for antibody ned by surface r a small subset o 1.7E-04 $sec^{-1}$]) a ntibodies can be is ed Fab molecule s between 2.9E and 1.7E-01 $sec^{-1}$.

## Biophy

For each nverted into human I oduced in research The

9.2, with no significant differences between Vκ and Vλ IgG1s (Fig. 13A). Purified human IgG1 yields in a transient HKB11 mammalian expression system ranged from 1 mg/L to more than 60 mg/L with an average expression level of 23 mg/L. Interestingly, Vλ IgG1s, with an average of 28 mg/L, showed significantly higher expression levels than Vκ IgG1s, with an average of 17 mg/L ($p < 0.0001$, t-test) (Fig. 13B). The aggregation propensity, as determined by HP-SEC experiments, was very low for the majority of binders. Of 259 tested IgG1 antibodies, 232 (89.6%) showed a monomer content equal to or higher than 90% and 196 (75.7%) had a monomer portion greater than 95% ( Fig. 13C). As an additional indicator for protein stability, the IgG1 melting temperatures were determined by DSF experiments. Of the tested IgGs, 233 (89.6%) had a melting temperature equal to or higher than the temperature corresponding to the unfolding of the Fc CH2 domain that occurs at about 68°C. The median Tm value of all Vκ IgG1 antibodies was significantly higher compared with the Vλ bearing IgG1s (70.9°C vs. 77.9°C, $p < 0.0001$, Mann–Whitney U-test) as shown in Figure 13D.

Figure 13. Biophysical features of selected Ylanthia IgG1 antibodies. (A) pI values, (B) production yields after purification, (C) monomer contents and (D) apparent melting temperatures of purified human Vκ (green) and Vλ (blue) IgG1 antibodies that were selected in various panning campaigns. In each panel the median with interquartile range is indicated. Grey shaded regions indicate the respective parameters preferred range th

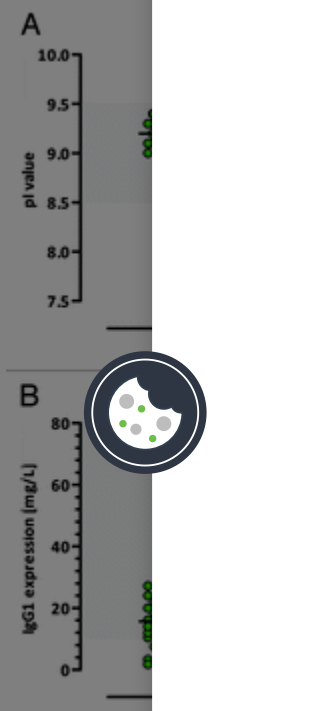

In conclusion, the majority of the selected IgG1 antibodies showed optimal biophysical characteristics that were comparable to the features initially determined for the corresponding VH/VL framework pairs.

## Discussion

In vitro display methods using recombinant libraries have been firmly established in the field of human antibody generation and are highly valued for their ability to deliver high affinity antibodies with tailor-made specificity. As large numbers of therapeutic antibody candidates have progressed from discovery through development, a great deal of knowledge has accumulated regarding the desired molecular properties of antibody drug candidates. Biophysical properties, such as thermodynamic stability and folding efficiency influence the solubility and aggregation behavior of antibodies. These features, therefore, are important factors in protein expression, manufacturing and formulation. Such features can also affect both pharmacokinetics and immunogenicity, altogether having important consequences for the therapeutic potential and the ease of use of an antibody.[56] Engineering to optimize the biophysical properties of any given candidate has therefore become an important aspect of antibody discovery. Rather than having to perform time and cost-intensive optimization, it would, however, be preferab With this goal in n been generate lanthia, a fully syn ermline VH/VL fr

Our visio ophysical proper inations of the h etween Ig heavy a nay enable the iden , 20 diverse segment cy in natural[3 d germline usage c the selected variable rity of the

both as Fab and IgG1. The rationale to look at Fab and IgG1 expression was that low expression levels often reflect sub-optimal folding properties.[58] High Fab display rates in turn are essential for successful phage selections because they maximize Fab–antigen interactions during phage selections. From this screening, 95 VH/VL pairs were selected for further in-depth characterization of expression and other biophysical characteristics in both Fab and IgG1 formats.

During manufacturing processes, therapeutic antibodies are subjected to a range of conditions that are likely to perturb their colloidal solubility and native conformation. We selected assays for further characterization of our framework VH/VL pairs to simulate those stress conditions and select for properties that ensure optimal performance. As an example, chemical stress is generated during virus inactivation by acid treatment that was meant to denature viral capsid proteins.[59,60] Low pH, however, destabilizes the antibody such that the processed protein eventually unfolds and denatures. To exclude VH/VL pairs that are sensitive to low pH, DSF and DLS experiments were performed to determine the apparent Tm and the hydrodynamic radius of purified VH/VL pairs under different pH conditions. The determination of the melting point provides a useful measure for protein stability and conformational integrity. In general, low Tm values indicate low stability of the VH/VL protein pair that might lead to higher aggregate levels in production batches, demanding increased efforts t[61] To further predict p uring formulat xtinction measure ab molecul and Ig light chain th

Through th superior biopl with sub-optima segments and 15 c the structura e occurren nly exceptio VH2, VH4 and Vκ4 le with scFv

to low display rates (unpublished observations; data not shown) and unfavorable biophysical characteristics of this framework.[19,48]

In contrast to earlier work that failed to reveal any evidence for preferences in natural pairing of particular VH and VL gene families,[39,62] it was recently suggested that the human VH1 family shows a strong pairing preference with the Vκ3 family.[57] Interestingly, two of the four VH1 family members within Ylanthia pair with Vκ3 members (i.e., VH1–18/Vκ3–20, VH1–46/Vκ3–15), indicating that this naturally occurring prevalence is reflected in favorable biophysical properties. Our observation of an increased tendency to aggregate for Vλ bearing VH/VL framework pairs (especially the Vλ3–1 framework) might be explained by their particularly low pI values or it could be an intrinsic feature of the primary sequence of the Vλ proteins. Isolated Vλ consensus sequences have been described to be relatively unstable by themselves with a tendency to dimerize, although scFv fragments containing Vλ domains were shown to possess partly very high stability due to a strong interaction between the VH and Vλ domains.[48] Furthermore, VH/VL pairings containing Vλ1 family members overall showed the lowest Tms, whereas VH/VL pairs with Vκ domains showed a tendency toward higher Tms. This might again be influenced by the generic amino acid composition of Vλ sequences, as well as the sequence and structural differences of Vλ and Vκ CDR-L3.[44,63]

The fully
h nucleotide
and ami
DR-Hs that
cover ge
e use of VH
sequenc
nt removal
of such
ally
immuno
eration of T
cell epit
rmed in a
cont
in E. coli
and in
uction of Fab
as well a

The maj
number of
function
DR-L3 and
CDR-H3s
n antigen-
binding
DR-L3

H3 cassettes were synthesized through the Slonomics technology.[29] While in nature, CDR-H3 length varies from a few amino acids to more than 30 residues,[53] only CDR-H3 lengths of 6 to 17 amino acids were implemented in Ylanthia, as these lengths represent the majority of naturally occurring CDR-H3 sequences. In addition, potential critical PTM sites have been omitted or reduced in the CDR3s to prevent later antibody heterogeneity, instability or even loss of function through post translational modifications.[64] Furthermore, the diversified CDR-L3 and CDR-H3 sequences were designed to obtain pI values ranging between 7.5 to 9 for the full-length antibody. This should maximize solubility of the protein in the neutral or slightly acidic formulation buffers routinely used. For antibodies with pI values greater than 9 rapid clearance from the blood and decreased half-life in vivo[65,66] have been described.

For the generation of Ylanthia, the diversified CDR-L3 and CDR-H3 cassettes were cloned consecutively into each of the 36 Ylanthia VH/VL pairs, without the use of an in-frame selection strategy, resulting in a total antibody library size of more than 1.3E+11 individual members. Thus, Ylanthia is 3-fold larger than the previously described HuCAL PLATINUM library[20] and equals the human PCR-derived CAT2.0 library[41] in size. To our knowledge, the quality of Ylanthia, with ~85% accurate clones is among the highest reported to date for recombinant antibody libraries. High-throughput 454 sequencing allowed for a precise and unbiased control of the library composition[43] and comparison to the in ed by 454 sequenc eration sequenc ple, a scFv library g que sequenc s of several Ig heavy sequences (Josef Pr rom naïve huma 24% to 31% uniq

To maint ablished for HuCAL G splay through Gs against recombi dentified in various p ready been acquire of

antibodies derived from Ylanthia and to underscore its potential to select for antibodies with preferred “processability” characteristics.

Among the selected binders, Vλ IgG1 antibodies yielded higher expression levels compared with Vκ bearing VH/VL IgG1 pairs. Interestingly, this difference observed following selection on a target had not been present in the initially tested 100 VH/VL pairs, indicating a potential influence of the selected CDR3s. Regarding monomer content, the behavior of the 36 VH/VL framework pairs (not more than 2% aggregates) is largely preserved in the VH/Vκ IgG1 output from phage pannings. As already discussed above for VH/Vλ pairs containing Vλ3–1, they seem to be more prone to aggregation. An explanation for this increased aggregation tendency may be found in the relatively flexible Vλ CDR-L3 compared with more rigid Vκ CDR-L3 sequence compositions.[44,63,69]

Nevertheless, the majority of the antigen-selected antibody molecules closely preserved the biophysical features that were characteristic of the corresponding “parental” VH/VL framework pair. Slight biophysical deviations were observed only in a minority of selected binders and thus have to be attributed to the influence of the particular CDR-L3 and CDR-H3 sequences. While such effects remain difficult to circumvent without abating overall CDR3 diversity, a very good balance between biophysi
selectio

The Yla
antibody
careful c
antibody
and fast
not re
proc

Materi

Evalua

To identify the most prevalent VH and VL gene segment pairs in the human Ig repertoire, various single B cell PCR studies from literature and from sampling of single human B cells in-house were evaluated.[30-35] Single cell sorts, Ig gene amplification and sequencing were basically performed as previously described.[5]

For CDR3 analysis, rearranged human antibody sequences were obtained from single B cell PCR experiments and from various Ig V-gene sequence databases such as V-BASE[70] and IgBLAST.[71] The amino acid sequences were imported into Microsoft Excel and CDR3 regions were analyzed by using custom-made Visual Basic utilities as described before.[19-21,72]

## Gene synthesis and assembly

V regions with flanking sites for restriction enzymes were synthesized by GeneArt with CDR-H3 (WGGDGFYAMDY) and kappa CDR-L3 (QQHYTTPPT) of the hu4D5–8 antibody[47] and lambda-like CDR-L3 (QSYDSSLSGVV) sequences[48] and the JH4, Jκ1 and Jλ2/3 germline protein sequences, respectively.[73-75] Codon usage optimization with respect to E. coli expression (avoiding rare human codons) and removal of potential cis-acting sequence motifs such as RNA instability motifs and cryptic splice donor and acceptor sites were performed by GeneArt.[27]

The synt the first
unique 5 nce to the
unique 3 er.
Upstrea enable
subsequ ne
sequenc the
modifie framework
region ( corporated
to en

## Biophy

The 20 V 8 Vλ region
construc Fab
expressi

First, po VH3-15

18, VH1–46, VH1–69, VH4–04, VH4–31, VH4–39, VH5–51, VH6–01) were inserted via the restriction sites for NheI and SalI, followed by insertion of the Vκ (Vκ1–05, Vκ1–06, Vκ1–09, Vκ1–12, Vκ1–16, Vκ1–17, Vκ1–27, Vκ1–39, Vκ3–20 Vκ3–11, Vκ3–15 and Vκ3–20) and Vλ (Vλ1–40, Vλ1–47, Vλ1–51, Vλ2–11, Vλ2–14, Vλ2–23, Vλ3–1 and Vλ3–21) pool with NdeI and Acc65I. For each step the ligation mixtures were electroporated into E.coli TOP10F' (Invitrogen).

From the resulting pYPdis10 and pJPx1_FH constructs, polyclonal DNA was prepared and transformed into electro-competent E. coli TOP10F′ (Invitrogen) for subsequent Fab display on filamentous M13 phage or TG1F$^{-}$ for bacterial Fab expression. Each transformed pYPdis10 and pJPx1_FH pool was plated on LB/Cam/Gluc plates and clones were picked into 384-well plates and stored in 15% glycerol ("master plates").

For identification of the respective VH/VL pair, clones were sequenced with Y_Fab_VH_for (5′-GATAAGCATGCGTAGGAGAAA-3′), Y_Fab_dis_VL_for (5-'TGTTGCCACCTTTATGTATG-3′) or Y_Fab_Bex_VL_for (5′-TGGAATTGTGAGCGGATAAC-3′).

## Small-scale phage preparations

Antibody phage preparations comprising the majority of the 400 VH/VL pairs were produced in small scale using 96-well plates. In brief, random clones from the master plates of
ated in 2× YT/Cam/
of 0.5 was reached
ged and re-suspend
mycin and 0.25 mM
rther incubate

## Relativ

Fab
body (Amersh
an anti-Fd antibody
utions of the phage su
peroxidase conjugat
splay rates for each
anti-M13. Titers we
ns.

Random clones from the 400 VH/VL pairs pool cloned in pJPx1 were inoculated in 2× YT/Cam/0.1% Gluc and incubated for at least 6 h at 30°C while shaking. Fab expression was induced by adding IPTG to a final concentration of 0.5 mM and incubated overnight at 22°C and with shaking. E. coli cells were lysed by adding 2× BBS/EDTA/lysozyme buffer (24.7 mg/ml boric acid, 18.7 mg/ml NaCl, 1.48 mg/ml EDTA, 2.5 mg/ml lysozyme, adjusted to pH 8.0 with 10 M NaOH) and subsequently blocked with 12.5% milk powder, 0.05% Tween® in PBS. Fab expression was determined by ELISA using an anti-human Fd capture antibody (The Binding Site) and an AP-labeled anti-FlagM2 (Sigma) detection antibody with AttoPhos (Roche). Relative Fab expression levels were calculated by dividing the signal of the respective Fab VH/VL pair through the signal of the reference Fab VH1–69/Vλ1–40 pair expressed with pMORPHx11.[20]

## Fab temperature stability ELISA

Appropriate dilutions of bacterial lysates were exposed to different temperatures (0°C, 60°C, 70°C and 80°C) for 45 min. Intact Fab molecules were detected by ELISA using an anti-6×His capture antibody (R&D Systems) and AP-labeled anti-human Ig kappa or anti-human Ig lambda (Sigma) detection antibodies with AttoPhos (Roche).

## Biophysical screening of IgG1 VH/VL pairs

For gene ments were sub-clon Vκ and 8 Vλ region fr pYMex2( 3 EBNA cells were gro 96-well plates u Invitrogen) with equ t chain expressi atants were harv

## Relativ

IgG1 exp LISA using a mouse a ntibody as biotin co elative IgG1 expressi H/VL pair

## CDR-L3 library synthesis by TRIM technology

Trinucleotide (Metkinen Chemistry) containing oligonucleotides were synthesized as previously described[21,28] in collaboration with ELLA Biotech. For synthesis of CDR-L3 cassettes, a total of 15 trimer-phosphoamidite-oligonucleotides with 24 unique, customized TRIMer mixtures were used to create diversity with an amino acid distribution close to that found in natural human rearranged antibodies. CDR-L3 cassettes were assembled and prepared with the appropriate restriction enzymes basically as described before.[20,21]

## CDR-H3 library synthesis by Slonomics technology

The synthesis of the diversified CDR-H3s was performed by using a modified version of the Slonomics technology (MorphoSys) for de novo gene synthesis.[29] The adapted procedure allowed the parallel incorporation of complex Anchor molecule mixtures and individual Anchor molecules during elongation reactions, permitting both the generation of variable and constant positions. For the synthesis of the CDR-H3s, a total of 18 different DNA fragments including length variations (from 6 to 17 variable positions) were generated. Using proprietary software, a list of Anchor mixtures with defined ratios and single Anchor molecules according to the amino acid distribution specifications of the CDR-H3 design was created and transferred to a robotic platform for auto esized by using th ursor molecul le sub-fragmen riction digest a erformed for each of t fragment and ana

## Bac

Electroc splay rates. Electroc at least 1E+10/μ procedures, E.coli XL selections phage w ere expresse

## Ylanthia vectors

The pMORPH30 and pMORPHx9 vectors[20] were used as templates for the generation of the new Fab CysDisplay pYPdis10 and Fab expression vectors pJPx1 and pYBex10, respectively, with the following modifications. To increase Fab display levels of the phagemid pYPdis10, codon usage optimization for gIII was performed by GeneArt[27] and a D23V mutation was introduced in gIIIp. For both vectors, the ompA and phoA leader sequences upstream of the Ig light and Ig heavy chain encoding sequences were modified at their C-termini to introduce the restriction sites NdeI and NheI, respectively, to assure authentic N-termini of the VL and VH protein sequences and to allow convenient sub-cloning of Fab fragments into pYMex10 or pYMex20 IgG vectors.

## Library cloning strategy

Prior to library cloning, the CDR-H3 and CDR-L3 areas of the 12 and 15 different VH and VL region sequences that comprise the finally selected 36 VH/VL pairs were replaced by an 823 bp and 488 bp stuffer fragment containing the β-lactamase and alkaline phosphatase gene, respectively. Stuffer sequences were cloned via BssHII and XhoI (CDR-H3) or BbsI and Acc65I (CDR-L3) into pYPdis10 to facilitate the vector preparations for library cloning.

At first, [redacted] library cassette[redacted]2, Vκ1–06/Vκ1–[redacted]-40/Vλ3–1 and clon[redacted]er transfor[redacted]TB medium, the num[redacted]uc agar plates. A[redacted]20-fold outgrow[redacted]600 of 1.8–2.0 v[redacted]repared (Qiagen)[redacted]s were the starting [redacted]

CDR-H3 [redacted] Slonomics technolo[redacted]es for BssHII and Xho[redacted]as described above.

## Library redundancy analysis and QC by 454 NGS

Quality control of the cloned libraries was performed by high throughput 454 sequencing using the GS Junior System (Roche). In general, amplicon 454 sequencing was performed according to the manuals provided by the manufacturer (GS Junior Titanium Series). Briefly, 4 amplicons of combined Ylanthia sub-libraries were produced by PCR [1 min 98°C, 15 cycles of 98°C for 15 sec, 60°C for 15 sec and 72°C for 15 sec, 72°C for 5 min, 15 ng template DNA, 0.4 µM of each primer, 200 µM dNTPs and 1 U Phusion polymerase (NEB)] using specific amplicon fusion primers. These ~50 nt oligonucleotides enclosed the adaptor A and B sequences, unique sequence tags (multiplex identifiers), as well as target-specific sequences. Agarose gel purified PCR products were further purified using AMPure beads (Beckman Coulter) and quantified by fluorometry using Quant-IT™ PicoGreen® reagent (Invitrogen). Amplicons were pooled, diluted and subjected to an emulsion PCR (emPCR) using the GS Junior Titanium Lib-A Kit (1 copy per bead). Beads were recovered and washed, and DNA positive beads were enriched. Roughly 500,000 enriched beads were deposited on a Pico Titer Plate and the sequencing run was performed as described in the manual.

Results from 454 sequencing were processed using the default amplicon signal processing feature of the GS Junior software package v2.5p1 to obtain high quality, filter pass
analyze
large se

## Large s

Phage p (Progen).
Phage ti Nanodrop,
peqlab)
LB/C

## Selecti

Equal ar r specific
antibody a “solid
phase pa (Nunc) and
a “Fc-ca c goat anti-

bound to streptavidin coated Dynabeads® (Dynal) and with eGFP, rhErbB4 and rhFZD-4 coupled to carboxy beads (Dynal) were performed according to standard protocols.[20,21,54,55] The Fab encoding inserts of the selected pYPdis10 phagemids were subcloned into the bacterial expression vector pYBex_Fab_FH to facilitate expression of soluble Fab in E. coli TG1F$^-$ cells and purification via a His6 tag.[55]

For screening purposes the recombinant antigens were coated onto MaxiSorp™ plates (Nunc) or Neutravidin microtiter plates and incubated with bacterial lysates containing Fab fragments. For detection of antigen-specific Fabs alkaline phosphatase (AP)-conjugated anti-human F(ab') 2 (Dianova) was applied in combination with AttoPhos (Roche). Fluorescence was measured at an excitation of 440 ± 25 nm and emission of 550 ± 35 nm.

## Expression and purification of His6-tagged Fab fragments in E. coli

Expression of unique binding Fab fragments in E. coli TG1F$^-$ cells was performed in 500 ml 2× YT cultures containing 34 µg/L Chloramphenicol and 0.1% (w/v) glucose shaken at 22°C until the $OD^{600}$ nm reached 0.5. Fab expression was induced by the addition of IPTG to a final concentration of 0.5 mM and further cultivation for 20 h at 22°C. Cells were harvested and disrupted using a freeze-thaw cycle followed by lysozyme treatment. His6-tagged Fab fragments were isolated via Profinity IMAC-Resin (Bio-Rad) and elut

Buffer ex columns (GE Healthca

concentr ab). The purity of 15% SDS-PAGE (Bi

## Con

To obtai in a two-step clo to the mamma e of the pcDNA3 the Ig light and Ig h

## Expres

Eukaryotic HKB11 cells[77] were transiently transfected with the expression vector pYMex10_h_IgG1. Cell culture supernatants were harvested at day 3 after transfection and IgG1 was purified via Protein A affinity chromatography (MabSelect SURE™, GE Healthcare). Buffer exchange was performed to PBS (pH 7.2, Invitrogen). IgG1 purity was analyzed under denaturing, reducing and non-reducing conditions in SDS-PAGE or by using LabChip® GX II (Caliper/Perkin Elmer). Purified IgG1 concentrations were determined by UV-spectrophotometry (Nanodrop, peqlab). Expression yields were calculated as amount of Protein A purified IgG1 per liter culture supernatant.

## Purified Fab and IgG1 thermal stability determination

The thermal stability of purified Fab fragments and IgG1 antibodies was determined by differential scanning fluorometry (DSF).[50-52] Diluted Sypro® Orange (Sigma) was added to each well of a 96-well iCycler iQ™ PCR Plate (Bio-Rad), and the Fab or IgG1 samples were tested at a final concentration of at least 0.1 mg/ml on an iQ5™ Thermal cycler (Bio-Rad). The temperature was scanned from 20–95°C at a heating rate of 60°C/h, and the melting temperature of unfolding was calculated by analysis of the inflection point of the fluorescence transition.

## Purified Fab and IgG1 monomer content determination

The mor determined by size e Superdex™ 75 HR 1( (Dionex, Thermo the column, separati vitrogen) as running m. For separati ence) was used on ic) in com for absolute molecul s injected onto the d recorded analyzin

## Purifie

The abili low pH

mg/ml with 1 M citrate buffer at pH 2.3 for 2.5 h and subsequent neutralization using 1 M Tris pH 9.0. Acid stressed and unstressed protein samples were characterized by DSF to evaluate the thermal stability, DLS to assess the hydrodynamic radius and polydispersity in solution, and UV/Vis measurements to determine the concentration of the proteins (280 nm) and the turbidity (320 nm).

## Statistics

The distributions of the data were tested for normality using the D'Agostino and Pearson omnibus test. For ease of interpretation, results of non-normally distributed variables are reported as non-transformed values and were analyzed by non-parametric two-tailed Mann–Whitney U-test. Gaussian-distributed parameters were analyzed by two-tailed Student t-test. Multi-group comparison for normally distributed data was performed by the analysis of variance with the Bonferroni post test. All tests were performed using GraphPad Prism® 5.02 software.

| Abbreviations: | | |
|---|---|---|
| mAbs | = | monoclonal antibodies |
| CDR | | |
| Fab | | |
| PTM | | |
| TRIM | | |
| Ig | | |

| | | |
|---|---|---|
| VH | = | variable Ig heavy chain region |
| VL | = | variable Ig light chain region |

## Supplemental material

### Additional material

Download Zip (182 KB) Additional material

## Acknowledgments

The authors gratefully acknowledge Tschimegma Bataagijn, Bernadette Gut, Angelika Geide, Christiane Huth, Jan Jaehrling, Tobias Neuber, Andrea Nudlbichler, Solveig Peters, Ingrid Pr partment, as well as f d support. We than d Jan Van den Brul also given to Kathrin L tion of figures a and Paul Wiegel f

## Disclos

All autho struction and data ncial involven ncial conflict with the those

Article contents | Related research

patent application, patent number WO2010136598, and T.T., I.S., Y.S. and S.U. have a pending patent application, patent number WO2012066129 and US20120129717.

HuCAL®, HuCAL GOLD®, HuCAL PLATINUM®, CysDisplay® and Ylanthia® are registered trademarks of MorphoSys AG. Slonomics® is a registered trademark of Sloning BioTechnology GmbH, a subsidiary of MorphoSys AG.

## Supplemental Material

Supplemental materials may be found here:

http://www.landesbioscience.com/journals/mabs/article/24218

# References


1. Carter PJ. Potent antibody therapeutics by design. Nat Rev Immunol 2006; 6:343 - 57; http://dx.doi.org/10.1038/nri1837; PMID: 16622479
PubMed | Web of Science ® | Google Scholar

2. Traggi R, et al. An efficie cells: potent neutra http://

3. Olsson ntibodies of pre 31; htt

4. Meijer al. Isolation of hun light chain pairing 6.02.040; PMID:

5. Tiller T, Meffre E, Yurasov S, Tsuiji M, Nussenzweig MC, Wardemann H. Efficient generation of monoclonal antibodies from single human B cells by single cell RT-PCR and expression vector cloning. J Immunol Methods 2008; 329:112 - 24; http://dx.doi.org/10.1016/j.jim.2007.09.017; PMID: 17996249

PubMed | Web of Science ® | Google Scholar

6. Tiller T. Single B cell antibody technologies. N Biotechnol 2011; 28:453 - 7; http://dx.doi.org/10.1016/j.nbt.2011.03.014; PMID: 21473940

PubMed | Web of Science ® | Google Scholar

7. Köhler G, Milstein C. Continuous cultures of fused cells secreting antibody of predefined specificity. Nature 1975; 256:495 - 7; http://dx.doi.org/10.1038/256495a0; PMID: 1172191

PubMed | Web of Science ® | Google Scholar

8. Lonberg N. Human monoclonal antibodies from transgenic mice. Handb Exp Pharmacol 2008; 69 - 97; http://dx.doi.org/10.1007/978-3-540-73259-4_4; PMID: 18071942

PubMed | Google Scholar

9. Hanes s by using riboso http://

10. He M, selection part ucleic Acids Re 396828

11. Boder olypeptide librari 697-553; PMID:

12. McCafferty J, Griffiths AD, Winter G, Chiswell DJ. Phage antibodies: filamentous phage displaying antibody variable domains. Nature 1990; 348:552 - 4; http://dx.doi.org/10.1038/348552a0; PMID: 2247164

PubMed | Web of Science ® | Google Scholar

13. Smith GP. Filamentous fusion phage: novel expression vectors that display cloned antigens on the virion surface. Science 1985; 228:1315 - 7; http://dx.doi.org/10.1126/science.4001944; PMID: 4001944

PubMed | Web of Science ® | Google Scholar

14. Winter G, Griffiths AD, Hawkins RE, Hoogenboom HR. Making antibodies by phage display technology. Annu Rev Immunol 1994; 12:433 - 55; http://dx.doi.org/10.1146/annurev.iy.12.040194.002245; PMID: 8011287

PubMed | Web of Science ® | Google Scholar

15. Marks JD, Hoogenboom HR, Bonnert TP, McCafferty J, Griffiths AD, Winter G. By-passing immunization. Human antibodies from V-gene libraries displayed on phage. J Mol Biol 1991; 222:581 - 97; http://dx.doi.org/10.1016/0022-2836(91)90498-U; PMID: 1748994

16. Vaugh t al. Human antibo ized phage displa 8/nbt0396-309; P

17. Hu Generation of a la e lambda. Scienc PMID: 25314

18. Hoet F Generation

complementarity-determining-region diversity. Nat Biotechnol 2005; 23:344 - 8; http://dx.doi.org/10.1038/nbt1067; PMID: 15723048

PubMed | Web of Science ® | Google Scholar

19. Knappik A, Ge L, Honegger A, Pack P, Fischer M, Wellnhofer G, et al. Fully synthetic human combinatorial antibody libraries (HuCAL) based on modular consensus frameworks and CDRs randomized with trinucleotides. J Mol Biol 2000; 296:57 - 86; http://dx.doi.org/10.1006/jmbi.1999.3444; PMID: 10656818

PubMed | Web of Science ® | Google Scholar

20. Prassler J, Thiel S, Pracht C, Polzer A, Peters S, Bauer M, et al. HuCAL PLATINUM, a synthetic Fab library optimized for sequence diversity and superior performance in mammalian expression systems. J Mol Biol 2011; 413:261 - 78; http://dx.doi.org/10.1016/j.jmb.2011.08.012; PMID: 21856311

PubMed | Web of Science ® | Google Scholar

21. Rothe C, Urlinger S, Löhning C, Prassler J, Stark Y, Jäger U, et al. The human combinatorial antibody library HuCAL GOLD combines diversification of all six CDRs according to the natural immune system with a novel display method for efficient selecti

http://

22. Ponse ability and functi . Molecules 2011; D: 21540796

23. Hooge . Nat Biotec 16151404

24. Hudso 9:395 - 402; http://

Article contents | Related research

25. Söderlind E, Strandberg L, Jirholt P, Kobayashi N, Alexeiva V, Aberg AM, et al. Recombining germline-derived CDR sequences for creating diverse single-framework antibody libraries. Nat Biotechnol 2000; 18:852 - 6; http://dx.doi.org/10.1038/78458; PMID: 10932154

PubMed | Web of Science ® | Google Scholar

26. Jenkins N, Murphy L, Tyther R. Post-translational modifications of recombinant proteins: significance for biopharmaceuticals. Mol Biotechnol 2008; 39:113 - 8; http://dx.doi.org/10.1007/s12033-008-9049-4; PMID: 18327554

PubMed | Web of Science ® | Google Scholar

27. Raab D, Graf M, Notka F, Schödl T, Wagner R. The GeneOptimizer Algorithm: using a sliding window approach to cope with the vast sequence space in multiparameter DNA sequence optimization. Syst Synth Biol 2010; 4:215 - 25; http://dx.doi.org/10.1007/s11693-010-9062-3; PMID: 21189842

PubMed | Google Scholar

28. Virnekäs B, Ge L, Plückthun A, Schneider KC, Wellnhofer G, Moroney SE. Trinucleotide phosphoramidites: ideal reagents for the synthesis of mixed oligonucleotides for rando
http://

29. Van de et al. A novel solid p s 2008; 45 :340 -

30. Mietzn eactive IgG memo rom nonre 105:9727 - 32; ht

Article contents | Related research

31. Tiller T, Tsuiji M, Yurasov S, Velinzon K, Nussenzweig MC, Wardemann H. Autoreactivity in human IgG+ memory B cells. Immunity 2007; 26:205 - 13; http://dx.doi.org/10.1016/j.immuni.2007.01.009; PMID: 17306569
PubMed | Web of Science ® | Google Scholar

32. Tsuiji M, Yurasov S, Velinzon K, Thomas S, Nussenzweig MC, Wardemann H. A checkpoint for autoreactivity in human IgM+ memory B cell development. J Exp Med 2006; 203:393 - 400; http://dx.doi.org/10.1084/jem.20052033; PMID: 16446381
PubMed | Web of Science ® | Google Scholar

33. Wardemann H, Yurasov S, Schaefer A, Young JW, Meffre E, Nussenzweig MC. Predominant autoantibody production by early human B cell precursors. Science 2003; 301:1374 - 7; http://dx.doi.org/10.1126/science.1086907; PMID: 12920303
PubMed | Web of Science ® | Google Scholar

34. Yurasov S, Hammersen J, Tiller T, Tsuiji M, Wardemann H. B-cell tolerance checkpoints in healthy humans and patients with systemic lupus erythematosus. Ann N.Y. Acad.Sci 2005; 1062:165 - 74; http://dx.doi.org/10.1196/annals.1358.019
PubMed | Web of Science ® | Google Scholar

35. Yurasc rsistent expres ; 203:2255 - 61; ht

36. Brezin ky PE. Ana and so M+ B cells. J Clin In D: 9153293

37. Dema sis of human VH ge tics 1995; 42:34

38. Foster SJ, Brezinschek HP, Brezinschek RI, Lipsky PE. Molecular mechanisms and selective influences that shape the kappa gene repertoire of IgM+ B cells. J Clin Invest 1997; 99:1614 - 27; http://dx.doi.org/10.1172/JCI119324; PMID: 9120005
PubMed | Web of Science ® | Google Scholar

39. de Wildt RM, Hoet RM, van Venrooij WJ, Tomlinson IM, Winter G. Analysis of heavy and light chain pairings indicates that receptor editing shapes the human antibody repertoire. J Mol Biol 1999; 285:895 - 901; http://dx.doi.org/10.1006/jmbi.1998.2396; PMID: 9887257
PubMed | Web of Science ® | Google Scholar

40. Chothia C, Lesk AM, Gherardi E, Tomlinson IM, Walter G, Marks JD, et al. Structural repertoire of the human VH segments. J Mol Biol 1992; 227:799 - 817; http://dx.doi.org/10.1016/0022-2836(92)90224-8; PMID: 1404389
PubMed | Web of Science ® | Google Scholar

41. Lloyd C, Lowe D, Edwards B, Welsh F, Dilks T, Hardman C, et al. Modelling the human immune response: performance of a 1011 human antibody repertoire against a broad panel of therapeutically relevant antigens. Protein Eng Des Sel 2009; 22:159 - 68; http://

42. Bhat N n B lymph bodies. Clin Exp In 1996.d01-733.x;

43. Glanvi deterr sight into the hu 6:20216 - 21; ht

44. Tomlinson IM, Cox JP, Gherardi E, Lesk AM, Chothia C. The structural repertoire of the human V kappa domain. EMBO J 1995; 14:4628 - 38; PMID: 7556106
PubMed | Web of Science ® | Google Scholar

45. Williams SC, Frippiat JP, Tomlinson IM, Ignatovich O, Lefranc MP, Winter G. Sequence and evolution of the human germline V lambda repertoire. J Mol Biol 1996; 264:220 - 32; http://dx.doi.org/10.1006/jmbi.1996.0636; PMID: 8951372
PubMed | Web of Science ® | Google Scholar

46. Dunn-Walters D, Boursier L, Spencer J. Effect of somatic hypermutation on potential N-glycosylation sites in human immunoglobulin heavy chain variable regions. Mol Immunol 2000; 37:107 - 13; http://dx.doi.org/10.1016/S0161-5890(00)00038-9; PMID: 10865109
PubMed | Web of Science ® | Google Scholar

47. Carter P, Presta L, Gorman CM, Ridgway JB, Henner D, Wong WL, et al. Humanization of an anti-p185HER2 antibody for human cancer therapy. Proc Natl Acad Sci U S A 1992; 89:4285 - 9; http://dx.doi.org/10.1073/pnas.89.10.4285; PMID: 1350088
PubMed | Web of Science ® | Google Scholar

48. Ewert
variab
2836(
han antibody
/S0022-

49. Steidl
hum
:1
maturation of
2008; 46
015

50. Cumm
of The
http://
pplications

51. Ericsson UB, Hallberg BM, Detitta GT, Dekker N, Nordlund P. Thermofluor-based high-throughput stability optimization of proteins for structural studies. Anal Biochem 2006; 357:289 - 98; http://dx.doi.org/10.1016/j.ab.2006.07.027; PMID: 16962548
PubMed | Web of Science ® | Google Scholar

52. He F, Hogan S, Latypov RF, Narhi LO, Razinkov VI. High throughput thermostability screening of monoclonal antibody formulations. J Pharm Sci 2010; 99:1707 - 20; PMID: 19780136
PubMed | Web of Science ® | Google Scholar

53. Zemlin M, Klinger M, Link J, Zemlin C, Bauer K, Engler JA, et al. Expressed murine and human CDR-H3 intervals of equal length exhibit distinct repertoires that differ in their amino acid composition and predicted range of structures. J Mol Biol 2003; 334:733 - 49; http://dx.doi.org/10.1016/j.jmb.2003.10.007; PMID: 14636599
PubMed | Web of Science ® | Google Scholar

54. Krebs B, Rauchenberger R, Reiffert S, Rothe C, Tesar M, Thomassen E, et al. High-throughput generation and engineering of recombinant human antibodies. J Immunol Methods 2001; 254:67 - 84; http://dx.doi.org/10.1016/S0022-1759(01)00398-2; PMID: 11406

55. Rauch t al. Human combi st the human - 205; http://

56. McGee pment 2007;
Goog

57. Jayara Protein Eng Des S : 22802295

58. Schaefer JV, Plückthun A. Transfer of engineered biophysical properties between different antibody formats and expression systems. Protein Eng Des Sel 2012; 25:485 - 506; http://dx.doi.org/10.1093/protein/gzs039; PMID: 22763265
PubMed | Web of Science ® | Google Scholar

59. Ejima D, Tsumoto K, Fukada H, Yumioka R, Nagase K, Arakawa T, et al. Effects of acid exposure on the conformation, stability, and aggregation of monoclonal antibodies. Proteins 2007; 66:954 - 62; http://dx.doi.org/10.1002/prot.21243; PMID: 17154421
PubMed | Web of Science ® | Google Scholar

60. Low D, O'Leary R, Pujar NS. Future of antibody purification. J Chromatogr B Analyt Technol Biomed Life Sci 2007; 848:48 - 63; http://dx.doi.org/10.1016/j.jchromb.2006.10.033; PMID: 17134947
PubMed | Web of Science ® | Google Scholar

61. Ahrer K, Buchacher A, Iberer G, Jungbauer A. Thermodynamic stability and formation of aggregates of human immunoglobulin G characterised by differential scanning calorimetry and dynamic light scattering. J Biochem Biophys Methods 2006; 66:73 - 86; http://dx.doi.org/10.1016/j.jbbm.2005.12.003; PMID: 16458360

62. Brezin variable heavy J Immunol 1998;
PubM

63. Luo ution of an :708 - 19; http://

64. Walsh apeutic protei t1252; PMID:

65. Zheng Y, Tesar DB, Benincosa L, Birnböck H, Boswell CA, Bumbaca D, et al. Minipig as a potential translatable model for monoclonal antibody pharmacokinetics after intravenous and subcutaneous administration. MAbs 2012; 4:243 - 55; http://dx.doi.org/10.4161/mabs.4.2.19387; PMID: 22453096

PubMed | Web of Science ® | Google Scholar

66. Igawa T, Ishii S, Tachibana T, Maeda A, Higuchi Y, Shimaoka S, et al. Antibody recycling by engineered pH-dependent antigen binding improves the duration of antigen neutralization. Nat Biotechnol 2010; 28:1203 - 7; http://dx.doi.org/10.1038/nbt.1691; PMID: 20953198

PubMed | Web of Science ® | Google Scholar

67. Ravn U, Gueneau F, Baerlocher L, Osteras M, Desmurs M, Malinge P, et al. By-passing in vitro screening--next generation sequencing technologies applied to antibody display and in silico candidate selection. Nucleic Acids Res 2010; 38:e193; http://dx.doi.org/10.1093/nar/gkq789; PMID: 20846958

PubMed | Web of Science ® | Google Scholar

68. Venet S, Ravn U, Buatois V, Gueneau F, Calloud S, Kosco-Vilbois M, et al. Transferring the ch to human antibo 71; http://

69. Kuroda R-L3 in antibo ce. Proteins 200 6

70. Retter atabase. Nuclei http://

71. Altschul SF, Madden TL, Schäffer AA, Zhang J, Zhang Z, Miller W, et al. Gapped BLAST and PSI-BLAST: a new generation of protein database search programs. Nucleic Acids Res 1997; 25:3389 - 402; http://dx.doi.org/10.1093/nar/25.17.3389; PMID: 9254694
PubMed | Web of Science ® | Google Scholar

72. Honegger A, Plückthun A. Yet another numbering scheme for immunoglobulin variable domains: an automatic modeling and analysis tool. J Mol Biol 2001; 309:657 - 70; http://dx.doi.org/10.1006/jmbi.2001.4662; PMID: 11397087
PubMed | Web of Science ® | Google Scholar

73. Hieter PA, Maizel JV Jr., Leder P. Evolution of human immunoglobulin kappa J region genes. J Biol Chem 1982; 257:1516 - 22; PMID: 6276389
PubMed | Web of Science ® | Google Scholar

74. Kawasaki K, Minoshima S, Nakato E, Shibuya K, Shintani A, Schmeits JL, et al. One-megabase sequence analysis of the human immunoglobulin lambda gene locus. Genome Res 1997; 7:250 - 61; http://dx.doi.org/10.1101/gr.7.3.250; PMID: 9074928
PubMed | Web of Science ® | Google Scholar

75. Ravet the human immu J and D genes 0400-1; PMID:

76. Stube man-specific qua primates. J Ph 009.01.030; PMID:

77. Cho M for recom http://

Download PDF

## Related research

People also read | Recommended articles | Cited by 151

### Information for

- Authors
- R&D professionals
- Editors
- Librarians
- Societies

### Opportunities

- Reprints and e-prints
- Advertising solutions
- Accelera
- Corporat

### Open access

- Overview
- Open journals
- Open Select
- Dove Medical Press
- F1000Research

### Help and information

- Help and contact
- Newsroom

Keep up

Register t
by email

Sig